IEEE Access
Multidisciplinary | Rapid Review | Open Access Journal

Received February 10, 2018, accepted March 26, 2018, date of publication April 13, 2018, date of current version May 24, 2018.

Digital Object Identifier 10.1109/ACCESS.2018.2826655

Use of a Rapid Method for Achieving Optimal Sensing Duration and Analysis of Data Rate Loss of Cognitive Radio Due to CLT

BIN GU[1,3], (Member, IEEE), TIECHENG SONG[1], (Member, IEEE), JING HU[1], (Member, IEEE), ZHENGQUAN LI[1,2], AND DAFEI SUN[1]

[1]National Mobile Communications Research Laboratory, Southeast University, Nanjing 210096, China
[2]State key Laboratory of Networking and Switching Technology, Beijing University of Posts and Telecommunications, Beijing 100876, China
[3]School of Electronic and Information Engineering, Nanjing College of Information technology, Nanjing 210023, China

Corresponding author: Tiecheng Song (songtc@seu.edu.cn)

This work was supported in part by the National Natural Science Foundation of China under Grant 61771126, Grant 61571108, and Grant 61372104, and in part by the Open Foundation of the State key Laboratory of Networking and Switching Technology, Beijing University of Posts and Telecommunications, under Grant SKLNST-2016-2-14.

ABSTRACT The central limit theorem (CLT)-based Gaussian approximation facilitates the probability analysis of cognitive radio (CR), but it incurs data rate loss due to the inaccurate configuration of the optimal sensing duration (OSD). To estimate the data rate loss, an approach to obtain a tight upper bound of the maximal achievable data rate over a Nakagami-m fading via-to-sense channel is proposed. Moreover, a direct formula is more desirable than an iteration scheme for a highly mobile CR that has to calculate the OSD more quickly. To meet this need, a strategy to achieve the OSD based on exponential interpolation is proposed. For Nakagami-Gamma shadowed fading via-to-sense channels, the proposed scheme is demonstrated to have advantages over the popularly utilized Hermite spline, such as: 1) a more tractable derivation of the probability density function (PDF) of the OSD and 2) a less complex calculation of the ergodic-sensing capacity. These advantages are significantly favorable for a CR network to achieve low latency communication and swiftly perform quality of service management to adapt to the high mobility.

INDEX TERMS Cognitive radio, CLT, Gaussian approximation, interpolation, PDF, spectrum sensing, optimal sensing duration.

I. INTRODUCTION

One of the important tasks for cognitive radio (CR) is sensing the environmental spectrum for opportunistic access. For a CR system, the fraction of the period of a data frame that is assigned to sensing will significantly impact its data throughput [1]–[5]. This issue involves the probability analysis of the detected signal, for which the Gaussian approximation based on the central limit theorem (CLT) enables mathematical tractability. However, this analysis inevitably leads to the inaccurate configuration of the optimal sensing duration (OSD) and the loss of data rates to a certain extent. Additionally, this issue involves a sensing-throughput tradeoff, for which a time-consuming optimization operation to achieve the OSD has to be performed [1]–[5]. Unfortunately, to the best of our knowledge, neither a tight upper bound of the maximal achievable data rate (MADR), which is applicable to estimate such a data rate loss, nor a direct formula replacing the conventional iteration scheme for the simplification of the calculation of the OSD have been found to date [1]–[5]. However, the two aforementioned needs have become unprecedentedly desirable, as the CR ability [6], tactile-latency [7] and high speed mobility [8] were raised as the requirements of the 5th Generation (5G) wireless network [6]–[8].

For a highly mobile CR system, its data frame and the fraction therein for the sensing have to be compressed. Thus, a question may arise as follows. Over a more limited size of the detected samples due to higher mobility, how much data rate will be lost due to applying the CLT? Moreover, higher mobility requires higher calculation speeds for the OSD. Next, another question may be raised as follows. Is a direct forward formula of OSD that is capable of replacing the traditional iteration scheme applicable?

Fortunately, for these two questions, our investigation indicates that although a closed-form formula of the exact MADR is not derivable due to a transcendental equation,

an upper bound of it is achievable if some skills are applied. Accordingly, the data rate loss due to the CLT can be estimated. Moreover, an interpolation approach based on the exponential interpolation (EI) to piecewisely fit the exact OSD is applicable. This approach's constraint equations are based on the coincidence of the functions at the starting end of each piece and that of their 1st order derivatives at both ends. We handle this analysis in this way in order to achieve a continuous probability density function (PDF) of the OSD as a whole of all the pieces. Such a scheme has two advantages over the conventional Hermite interpolation (HI) [9], [10], which also keeps the continuity of the 1st order derivatives. They are that: a) it renders the derivation of the PDF of the OSD tractable due to ease of deriving the inverse function of the OSD vs. the SNR, and b) it significantly decreases the complexity of the computation of the ergodic capacity over the via-to-sense fading channel. For the cross-layer QoS management of a wireless network, the resource allocation (RA), the call admission control (CAC) [11], [12], and the frame alignment [25] have to be performed in a timely manner. Thus, the quick awareness of such information becomes significantly favourable for the CRs at high mobility.

The remainder of this paper is organized as follows. In section III, the addressed problem is formulated. Section IV and V provide several related theoretical analyses and derivations. Section VI presents the simulation verifications followed by Section VII, where all conclusions are drawn.

II. KEY ABBREVIATIONS

For more convenient referencing, the key abbreviations are listed in Tab. 1.

TABLE 1. Key abbreviations in an alphabetical order.

Abbr.	Full Name
CAC	Call Admission Control
CDF	Cumulative Distribution Function
CDRL	CLT-resultant Data Rate Loss
CIDR	CLT-resultant Imaginary Date Rate
CIOSD	CLT-resultant Imaginary OSD
CLT	Central Limit Theorem
CMADR	CLT-resultant MADR
CPDR	CLT-resultant Physically occurring Date Rate
CR	Cognitive Radio
CSCG	Circular Symmetric Complex Gaussian
EI	Exponential Interpolation
EDR	Exact Data Rate
EMADR	Exact MADR
EOSD	Exact OSD
i.i.d.	independent identical distribution
GS	Golden Section (optimization method)
HI	Hermite Interpolation
LOS	Line of Sight
LLC	Low Latency Communication
MADR	Maximal Achievable Data Rate
NESC	Normalized Ergodic Sensing Capacity
OFDMA	Orthogonal Frequency Division Multiple Access
OSD	Optimal Sensing Duration
PDF	Probability Density Function
QoS	Quality of Service
RA	Resource Allocation
RV	Random Variable
PSK	Phase Shift Keying (digital modulation)
RV	Random Variable
SER	Symbol Error Rate
SNR	Signal to Noise Ratio
TTI	Transmission Time Interval

III. MATHEMATICAL FORMULATION

A. OPTIMAL SENSING DURATION AND MAXIMAL ACHIEVABLE DATA RATE OF COGNITIVE RADIO

For the energy detection based spectrum sensing approach, the statistical test result based on a set of detected samples can be expressed as [1]

$$t(\mathbf{Y}) = \frac{1}{K}\sum_{k=1}^{K} |y(k)|^2 \tag{1}$$

where

$$\mathbf{Y} = \{y(k) | y(k) = s(k) + z(k),\ k \in \mathbf{K}\}, \tag{2}$$

Also, k and $\mathbf{K}$ represent the sample-index and the set including those indices with cardinality of K, respectively. $K = f_s\tau$, where f_s and τ are the sampling rate and sensing duration, respectively. $y(k)$ is the kth sample for testing. $s(k)$ and $z(k)$ are the nth items of the signal and noise sample-sets that are mutually independent with variances of σ_s^2 and σ_z^2, respectively. $z(k) \sim \mathrm{CN}(0, \sigma_z^2)$ (i.e., it follows a circular symmetric complex Gaussian (CSCG) distribution with mean of 0 and variance of σ_z^2) [13], [14]. For a sensing operation via a Nakagami-m fading channel, the conditional probability density function (PDF) of the instantaneous signal to noise ratio (SNR) is given as follows [14], [15]

$$f_{\dot{\gamma}}(x|\gamma) = \frac{1}{\Gamma(m)}\left(\frac{m}{\gamma}\right)^m x^{m-1} e^{\left(-\frac{m}{\gamma}x\right)}, \quad x \geq 0,\ m \geq 1/2 \tag{3}$$

where m is the Nakagami fading parameter. A smaller m results in more severe multipath fading. $m = 1/2$, $m = 1$, $m > 1$ and $m = \infty$ represent the single-side Gaussian, Rayleigh, Rician and line of sight (LOS) channels, respectively [14], [15]. $\Gamma(\cdot)$ denotes the Gamma function [13], [23], $\dot{\gamma}$ is the instantaneous SNR, and γ is the mean of $\dot{\gamma}$ defined as $\gamma = \sigma_s^2/\sigma_z^2$. Formula (3) indicates that $\dot{\gamma} \sim \mathrm{Ga}(m, \gamma/m)$, where the sign '$\sim$' denotes 'follow' and $\mathrm{Ga}(k, \theta)$ as a generic sign represents the Gamma distribution with k and θ being its shape and scale parameter, respectively [13], [23].

Obviously, γ is also a random variable (RV) in the sense of longer term fading due to the path loss or shadowing [14]. For the simplification of analysis, the path loss in this instance is assumed to be constant during sensing. Thus, γ usually meets a logarithm Gaussian distribution [13], [14]. For the ease of mathematical handling, it is typical to employ the Gamma distribution as its approximate alternative, the PDF of which

is given by [16].

$$f_{\gamma}(y|\bar{\gamma}) = \frac{y^{M-1}}{\Gamma(M)\,\bar{\gamma}^{M}} \exp\left(-\frac{y}{\bar{\gamma}}\right), \quad y \geq 0,\ M \geq 1/2 \quad (4)$$

where M is a parameter inverse-proportionally reflecting the severity of shadow fading and $\bar{\gamma}$ is a parameter identical to the mean of γ (i.e., the mean SNR of shadow fading). An overall view of Eqs. (3) and (4) suggests that $\dot{\gamma}$ experiences a Nakagami-Gamma shadowed fading [16], the PDF of which, if taking the form of $f_{\dot{\gamma}}(x \mid \bar{\gamma})$, will contain the modified Bessel function of the second kind known as the generalized-K model [22].

Let us focus on the context that the licensed (i.e., primary) signal does not vary so fast that it is considered to be a constant during sensing. It propagates via an aforementioned fading channel to arrive at the detector of a cognitive (i.e., secondary) system. Therefore, the variation of $s(k)$ depends only on the channel. The temporal spacing of $s(k), k = 1 \cdots K$ is sufficient so that they can be viewed as uncorrelated. Either $z(k)$ or $s(k), k = 1 \cdots K$ have an independent identical distribution (i.i.d.).

Under hypothesis $\mathcal{H}_0$ (i.e., $s(k) = 0, k = 1 \cdots K$), $t(\mathbf{Y})$ of (1) can be rewritten as

$$t(\mathbf{Y}|\mathcal{H}_0) = t(\{z(k), k \in \mathbf{K}\}) = \frac{1}{K}\sum_{k=1}^{K} |z(k)|^2 \quad (5)$$

which follows the Chi-square distribution with a degree of freedom of $2K$ if $\sigma_z^2 = 1$ [13], a special case of Gamma distribution. Here, we still regard it as Gamma distributed, represented as [13]

$$t(\mathbf{Y}|\mathcal{H}_0) \sim \mathrm{Ga}\left(K, \sigma_z^2/K\right). \quad (6)$$

In the other case of hypothesis, $\mathcal{H}_1$ (i.e., $s(k) \neq 0$, $k = 1 \cdots K$) $t(\mathbf{Y})$ of (1) can be rewritten as

$$t(\mathbf{Y}|\mathcal{H}_1) = t(\{y(k), k \in \mathbf{K}\}) = \frac{1}{K}\sum_{k=1}^{K} |s(k) + z(k)|^2 \quad (7)$$

which is also observed to be Gamma distributed. Therefore, a proposition needs to be proposed as follows.

Proposition 1: The probability of $t(\mathbf{Y}|\mathcal{H}_1)$ of (7) is Gamma distributed, represented as

$$t(\mathbf{Y}|\mathcal{H}_1) \sim \mathrm{Ga}(\kappa, \theta) \quad (8)$$

where κ and θ are given by

$$\kappa = K\xi(m, \gamma), \quad (9.a)$$

$$\theta = \frac{\sigma_z^2(1+\gamma)}{K\xi(m, \gamma)} \quad (9.b)$$

and $\xi(m, \gamma)$ is given by

$$\xi(m, \gamma) = \frac{(1+\gamma)^2}{\gamma^2/m + 2\gamma + 1}. \quad (9.c)$$

Proof: See Appendix A.

The mean and variance of $t(\mathbf{Y} \mid \mathcal{H}_1)$ of (7) (denoted $\mu_{\mathcal{H}_1}$ and $\sigma^2_{\mathcal{H}_1}$, respectively) are also derivable (see Appendix A) based the corresponding formulae of Gamma distribution [13], given by

$$\mu_{\mathcal{H}_1} = \kappa\theta = (1+\gamma)\sigma_z^2, \quad (10.a)$$

$$\sigma^2_{\mathcal{H}_1} = \kappa\theta^2 = \frac{(1+\gamma)^2\sigma_z^4}{K\xi(m, \gamma)}. \quad (10.b)$$

Similarly, for $t(\mathbf{Y} \mid \mathcal{H}_0)$, its mean and variance are given by

$$\mu_{\mathcal{H}_0} = \sigma_z^2, \quad (11.a)$$

$$\sigma^2_{\mathcal{H}_0} = \sigma_z^4/K. \quad (11.b)$$

Substituting $m = 1$ and $m \to \infty$ into (10.b) yields $\sigma^2_{\mathcal{H}_1} = \sigma_z^4(\gamma+1)^2/K$ and $\sigma^2_{\mathcal{H}_1} = \sigma_z^4(2\gamma+1)/K$, coinciding with the 3rd and 1st cases of (8) of [1], respectively. Thus, formula (10) provides a more general form than [1].

Let p_{d} denote the detection probability that the CR system detects the presence of a licensed signal while it is indeed active, and p_{f} is the false alarm probability such that the CR system falsely declares the presence of the licensed signal in its absence. In [1], it focuses on a context in which the signal is complex PSK-modulated and is propagated along a LOS path while the noise is CSCG distributed. This paper is focused on a new context in which the licensed system's transmitted signal does not vary significantly within the cognitive system's sensing duration so that it can be considered invariant. Nevertheless, it goes through a Nakagami-Gamma shadowed fading channel prior to its arrival. In such a new context, let us re-derive p_{d} and p_{f} as follows.

Based on proposition 1, the PDF of $t(\mathbf{Y} \mid \mathcal{H}_1)$ is given by

$$f_{t(\mathbf{Y}|\mathcal{H}_1)}(x) = \frac{x^{\kappa-1}}{\Gamma(\kappa)\,\theta^{\kappa}} \exp\left(-\frac{x}{\theta}\right), \quad x \geq 0. \quad (12)$$

Accordingly, p_{d} is derivable to be

$$\begin{aligned} p_{\mathrm{d}}(m, \gamma, \varepsilon) &= \int_{\varepsilon}^{\infty} f_{t(\mathbf{Y}\mid\mathcal{H}_1)}(x)\,\mathrm{d}x \\ &= \frac{1}{\Gamma(\kappa)}\int_{\varepsilon/\theta}^{\infty}\left(\frac{x}{\theta}\right)^{\kappa-1}\exp\left(-\frac{x}{\theta}\right)\mathrm{d}\frac{x}{\theta} = \frac{\Gamma(\kappa, \varepsilon/\theta)}{\Gamma(\kappa)} \\ &= \Gamma_0(\kappa, \varepsilon/\theta) = \Gamma_0\left(K\xi(m, \gamma), \frac{\varepsilon K\xi(m, \gamma)}{\sigma_z^2(1+\gamma)}\right) \end{aligned} \quad (13)$$

where $\Gamma(\cdot, \cdot)$ denotes the upper incomplete Gamma function, $\Gamma_0(\cdot, \cdot)$ is its regularized form [13], [23], and ε is the decision threshold for the detection of the result. Formula (13) indicates that p_{d} depends on the three parameters of m, γ and ε.

To limit the CR's interference in the licensed system under a specified level, it is usually required that $p_{\mathrm{d}} \geq p_{\mathrm{d0}}$, where p_{d0} is termed as the minimal detection probability. The substitution of eq. (13) into $p_{\mathrm{d}} \geq p_{\mathrm{d0}}$ leads to

$$\begin{aligned} \varepsilon &\leq \varepsilon_0(\gamma, m, p_{\mathrm{d0}}) \\ &= \theta\Gamma_0^{-1}(\kappa, p_{\mathrm{d0}}) = \frac{\sigma_z^2(1+\gamma)}{K\xi(m, \gamma)}\Gamma_0^{-1}(K\xi(m, \gamma), p_{\mathrm{d0}}) \end{aligned} \quad (14)$$

where ε_0 is the upper limit of ε and $\Gamma_0^{-1}(\cdot, \cdot)$ denotes the inverse function of $\Gamma_0(\cdot, \cdot)$. The above formula indicates the dependence of ε_0 on the parameters of γ, m and p_{d0}.

As a result of (6), the PDF of $t\left(\mathrm{Y} \mid \mathcal{H}_0\right)$ is derived to be

$$f_{t(\mathbf{Y} \mid \mathcal{H}_0)}(x)=\frac{x^{K-1}K^K}{\Gamma(K)\left(\sigma_z^2\right)^K}\exp\left(-\frac{Kx}{\sigma_z^2}\right),\quad x\geq 0. \tag{15}$$

Therefore, the p_{f} over ε_0 becomes derivable, given by

$$\begin{aligned}&p_{\mathrm{f}}\left(\tau,\sigma_z^2,\varepsilon_0\right)\\&=\int_{\varepsilon_0}^{\infty}f_{t(\mathbf{Y}|\mathcal{H}_0)}(x)\,\mathrm{d}x\\&=\frac{1}{\Gamma(K)}\int_{K\varepsilon_0/\sigma_z^2}^{\infty}\left(\frac{x}{\sigma_z^2/K}\right)^{K-1}\exp\left(-\frac{x}{\sigma_z^2/K}\right)\mathrm{d}\frac{x}{\sigma_z^2/K}\\&=\frac{\Gamma\left(K,K\varepsilon_0/\sigma_z^2\right)}{\Gamma(K)}=\Gamma_0\left(K(\tau),\frac{K(\tau)\varepsilon_0(\gamma,m,p_{\mathrm{d0}})}{\sigma_z^2}\right).\end{aligned} \tag{16}$$

Since $K=f_{\mathrm{s}}\tau$, formula (16) implies that the four parameters of p_{d0}, τ, γ and m will impact the p_{f} along with f_{s} and σ_z^2 that are usually configured or considered to be fixed. The former two (p_{d0} and τ) are usually programmable, while the latter two (γ and m) are determined merely by the radio circumstance. Thus, in order to clarify such dependencies, let us rewrite (16) using a more dependence-shown formula as follows.

$$p_{\mathrm{f}}(p_{\mathrm{d0}},\tau,\gamma,m)=\Gamma_0\left(K(\tau),\frac{K(\tau)\varepsilon_0(\gamma,m,p_{\mathrm{d0}})}{\sigma_z^2}\right) \tag{17}$$

Based on the well-known central limit theorem (CLT) [13], it can be stated that

$$t\left(\mathbf{Y} \mid \mathcal{H}_0\right)\dot{\sim}\,\mathcal{N}\left(\mu_{\mathcal{H}_0},\sigma_{\mathcal{H}_0}^2\right), \tag{18}$$

$$t\left(\mathbf{Y} \mid \mathcal{H}_1\right)\dot{\sim}\,\mathcal{N}\left(\mu_{\mathcal{H}_1},\sigma_{\mathcal{H}_1}^2\right), \tag{19}$$

where the symbol $\dot{\sim}$ denotes 'approximately follows', and $\mathcal{N}\left(\mu,\sigma^2\right)$ as a generic symbol denotes the normal (i.e., Gaussian) distribution with μ and σ^2 being its mean and variance, respectively.

The PDF formula of the normal distribution is well-known. Accordingly, an approximate decision threshold for $t\left(\mathbf{Y} \mid \mathcal{H}_1\right)$ to meet the p_{d0} is easily derived, given by

$$\hat{\varepsilon}_0=\mu_{\mathcal{H}_1}+\sigma_{\mathcal{H}_1}\mathrm{Q}^{-1}(p_{\mathrm{d0}}) \tag{20}$$

where $\mathrm{Q}^{-1}(\cdot)$ denotes the inverse of the Q function given by $\mathrm{Q}(x)=\left(1/\sqrt{2\pi}\right)\int_x^{\infty}e^{-\frac{t^2}{2}}\mathrm{d}t$ [13].

Consequently, the second type of false alarm probability (in a sense other than that of p_{f} of (17)) is obtained using $\hat{\varepsilon}_0$ and $\mathcal{N}\left(\mu_{\mathcal{H}_0},\sigma_{\mathcal{H}_0}^2\right)$ as two approximate alternatives. It is given by

$$\hat{p}_{\mathrm{f}}=\mathrm{Q}\left(\frac{\hat{\varepsilon}_0-\mu_{\mathcal{H}_0}}{\sigma_{\mathcal{H}_0}}\right). \tag{21}$$

By replacing $\hat{\varepsilon}_0$ with (20) [therein $\mu_{\mathcal{H}_1}$ and $\sigma_{\mathcal{H}_1}$ are further replaced with (10.a) and (10.b), respectively], $\mu_{\mathcal{H}_0}$ and $\sigma_{\mathcal{H}_0}$ with (11.a) and (11.b), respectively, it turns into

$$\hat{p}_{\mathrm{f}}(p_{\mathrm{d0}},\tau,\gamma,m)=\mathrm{Q}\left(\mathrm{Q}^{-1}(p_{\mathrm{d0}})\sqrt{\gamma^2/m+2\gamma+1}+\gamma\sqrt{K(\tau)}\right). \tag{22}$$

It is still worthy to remind you that from a strict point of view, $t\left(\mathbf{Y} \mid \mathcal{H}_0\right)$ of (5) fluctuates on the law of Gamma distribution as (6) indicates rather than the normal distribution as (18) does. Thus, the $\hat{p}_{\mathrm{f}}$ of (21) does not reflect the exact false alarm probability that actually occurs in the physical layer. Therefore, it is still necessary to present such a false alarm probability in a sense distinct from the two that were discussed, which is obtained based on (20) and (6). We denote it by $\tilde{p}_{\mathrm{f}}$ and represent it as

$$\tilde{p}_{\mathrm{f}}=\frac{1}{\Gamma(K)}\int_{K\hat{\varepsilon}_0/\sigma_z^2}^{\infty}\zeta^{K-1}e^{-\zeta}d\zeta. \tag{23}$$

To clarify the major dependent variables of $\tilde{p}_{\mathrm{f}}$, we derive it into the form of

$$\tilde{p}_{\mathrm{f}}(p_{\mathrm{d0}},\tau,\gamma,m)=\Gamma_0\left(K(\tau),\frac{K(\tau)\hat{\varepsilon}_0\left(\mu_{\mathcal{H}_1}(\gamma,m),\sigma_{\mathcal{H}_1}(\gamma,m),p_{\mathrm{d0}}\right)}{\sigma_z^2}\right). \tag{24}$$

Therefore, for a CR system, there exist three types of data rates corresponding to (17), (22) and (24), respectively, as follows.

a) The *Exact Data Rate* (*EDR*), which is based on an exact decision threshold and an exact PDF of $t\left(\mathbf{Y} \mid \mathcal{H}_0\right)$, is given by

$$B(\tau,\gamma)=\left(1-\frac{\tau}{T}\right)(1-p_{\mathrm{f}}) \tag{25}$$

where B denotes the data rate normalized to that of the non-CR case, T is the period of a data frame, and $(1-\tau/T)$ denotes the other part of T than τ for the transmission of the CR's own data provided that the detection results indicate the absence of the licensed signal [1].

b) The *CLT-resultant Physically occurring Date Rate* (*CPDR*), which treats $\hat{\varepsilon}_0$ as an approximate alternative of ε_0, is given by

$$\tilde{B}(\tau,\gamma)=\left(1-\frac{\tau}{T}\right)(1-\tilde{p}_{\mathrm{f}}). \tag{26}$$

c) The *CLT-resultant imaginary date rate* (*CIDR*) is also based on $\hat{\varepsilon}_0$ to detect $t\left(\mathbf{Y} \mid \mathcal{H}_0\right)$, the distribution of which is actually Gamma but is regarded by CR as Normal. In other words, CIDR is a type of data rate that never occurs in the physical layer. Let this data rate be expressed as

$$\hat{B}(\tau,\gamma)=\left(1-\frac{\tau}{T}\right)\left(1-\hat{p}_{\mathrm{f}}\right). \tag{27}$$

Based on the data rates in different senses as above, there may be two types of OSDs as follows.

a) The *Exact OSD* (*EOSD*), which depends on (25), is given by

$$\tau_0(\gamma)=\underset{0\leq\tau\leq T}{\operatorname{argmax}}\ B(\tau,\gamma). \tag{28}$$

b) The *CLT-resultant imaginary OSD* (*CIOSD*), which is based on (27), is represented as

$$\hat{\tau}_0(\gamma) = \underset{0\le\tau\le T}{\operatorname{argmax}}\ \hat{B}(\tau,\gamma). \tag{29}$$

Correspondingly, further based on the types of OSDs defined as above, two MADR-related concepts are defined as follows.

a) The *Exact MADR* (*EMADR*), which is determined by (28) and (17), is given by

$$B_0(\gamma) = \left(1 - \frac{\tau_0(\gamma)}{T}\right)(1 - p_{\mathrm{f}}). \tag{30}$$

b) The *CLT-resultant MADR* (*CMADR*), which is determined by (29) and (24), is given by

$$\tilde{B}_0(\gamma) = \left(1 - \frac{\hat{\tau}_0(\gamma)}{T}\right)(1 - \tilde{p}_{\mathrm{f}}). \tag{31}$$

Therefore, the *CLT-resultant Data Rate Loss* (*CDRL*) that can be defined as $\Delta B_0(\gamma) = B_0(\gamma) - \tilde{B}_0(\gamma)$. It is further expanded to be

$$\Delta B_0(\gamma) = \left(1 - \frac{\tau_0(\gamma)}{T}\right)(1 - p_{\mathrm{f}}) - \left(1 - \frac{\hat{\tau}_0(\gamma)}{T}\right)(1 - \tilde{p}_{\mathrm{f}}) \tag{32}$$

B. RAISE OF QUESTIONS

Facing formula (32), three interesting questions are raised as follows.

The 1st question: Under the context of high mobility, how significant the magnitude of CDRL of (32) will be?

Under the context of high mobility, the CR data frame has to be compressed for two reasons as follows. First, the licensed signal's rapid alternation between emergence and vanishment becomes very likely, thereby compelling the detection of its availability to be performed more frequently. To adapt to such a scenario, the data frame has to be shorter. This phenomenon will become more severe if the user's devices shuttle rapidly through buildings. Second, the channel estimation for the CR system's own communication also needs to occur more frequently due to the faster variation of the channel.

As a result, the sensing time slot within a data frame will be squeezed, leading to a more limited size of samples for detection. This means a larger error of optimization for the MADR due to applying the CLT. Therefore, the 1st question arises as above.

The 2nd question: For the solution of (28), is a direct formula that can replace the conventional iteration scheme applicable? If so, such a formula will be more suitable to the high mobility since its related operation saves more time.

In an effort to solve such a problem as (28) gives, one usually resorts to the iteration-based numerical approach. This is indeed a feasible scheme under a stationary or quasi-stationary context. Nevertheless, for high mobility, the availability of spectrum holes varies so rapidly that the iteration-based calculation may be incapable of keeping up with such a rapid variation. Under this scenario, raising the 2nd question becomes valuable.

The 3rd question: In the context of high mobility, is the statistical information of the OSD and MADR quickly acquirable by the CR that is detecting the licensed signal through an ergodically fading channel?

In such a case, the quick acquisition of such information becomes significantly important, since those cross-layer QoS managements (e.g., the resource allocation (RA), the call admission control (CAC) [11], [12], and the frame alignment [25]) are required to be finished within a demanding latency [7]. Thus, the 3rd question is highlighted.

For the 1st question, fortunately, our investigation in the next section will show that although a closed-form formula representing (28) is never derivable, an upper bound of it is achievable if some skill is applied. On this basis, the data rate loss due to the CLT resultant error can be estimated. The verifying simulation test in section VI indicates that such a date rate loss is still acceptable, provided that the related parameters are configured within the range regulated by IEEE 802.16e [19].

Regarding the 2nd question, our works in subsection V.B and section VI indicate that a forthright and convenient formula, based on the exponential interpolation to approximate the exact OSD will become an effective tool.

Facing the 3rd question, subsections V.C and VI will demonstrate that in an approximation sense, the probability density functions (PDF) of the OSD and MADR are achievable if applying some skills.

IV. DATE RATE LOSS DUE TO CLT-BASED APPROXIMATION

Reference [1] has proved that $\hat{B}(\tau,\gamma)$ of (27) is concave with respect to (w. r. t.) τ if $\hat{p}_{\mathrm{f}} \le 0.5$, and the following proposition 4 will indicate that $B(\tau,\gamma)$ of (25) w. r. t. τ is also concave if $p_{\mathrm{f}} \le 0.5$. Thus, the closed-form formula expressing (28) inevitably involves solving the equations such that $\partial B(\tau,\gamma)/\partial\tau = 0$. The solution of such an equation involves transcendental functions that disables (28) to be expressed in a closed form [17]. Similarly, the closed formed formula expressing (30) is also unachievable, and neither is (32).

However, a tight upper bound of (30) (although it still needs tiny recursion operations) is attainable. Such a bound can be supported by a proposition as follows.

Proposition 2: For the EMADR given by (30), an upper bound denoted $\mathcal{B}_0$ is achievable (i.e., $B_0(\gamma) \le \mathcal{B}_0(\gamma)$). $\mathcal{B}_0$ is given by (33.a), as shown at the top of the next page, where $B(\tau,\gamma)$ is given by (25). Meanwhile, $B'_\tau(\tau,\gamma)$ is given by

$$B'_\tau(\tau,\gamma) = -\frac{1-p_{\mathrm{f}}}{T} - \left(1 - \frac{\tau}{T}\right)\frac{\partial p_{\mathrm{f}}(\tau,\gamma)}{\partial\tau} \tag{33.b}$$

in which

$$\frac{\partial p_{\mathrm{f}}}{\partial\tau} = \frac{\Gamma'_\tau\left(K, K\varepsilon_0/\sigma_z^2\right)\Gamma(K) - \Gamma\left(K, K\varepsilon_0/\sigma_z^2\right)\Gamma'_\tau(K)}{\Gamma^2(K)} \tag{33.c}$$

$$\mathcal{B}_0(\gamma) = \frac{B'_\tau(\acute{\tau},\gamma)B(\grave{\tau},\gamma) - B'_\tau(\grave{\tau},\gamma)B(\acute{\tau},\gamma) + B'_\tau(\acute{\tau},\gamma)B'_\tau(\grave{\tau},\gamma)(\acute{\tau}-\grave{\tau})}{B'_\tau(\acute{\tau},\gamma) - B'_\tau(\grave{\tau},\gamma)} \tag{33.a}$$

$$\dot{\tau}^{(i)} = \frac{B(\grave{\tau}^{(i-1)},\gamma) - B(\acute{\tau}^{(i-1)},\gamma) + \acute{\tau}^{(i-1)}B'_\tau(\acute{\tau}^{(i-1)},\gamma) - \grave{\tau}^{(i-1)}B'_\tau(\grave{\tau}^{(i-1)},\gamma)}{B'_\tau(\acute{\tau}^{(i-1)},\gamma) - B'_\tau(\grave{\tau}^{(i-1)},\gamma)} \tag{34.f}$$

where $\Gamma'_\tau\left(K, K\varepsilon_0/\sigma_z^2\right)$ and $\Gamma'_\tau(K)$ are given by (B.3.1) and (B.2) in Appendix B, respectively.

Meanwhile, $\acute{\tau} = \acute{\tau}^{(i)}, \grave{\tau} = \grave{\tau}^{(i)}$ where $\acute{\tau}^{(i)}$ and $\grave{\tau}^{(i)}$ are the results of a set of recursive formulae[1] as follows

$$\begin{cases} \acute{\tau}^{(i)} = \dot{\tau}^{(i)} \\ \grave{\tau}^{(i)} = \grave{\tau}^{(i-1)} \end{cases} \quad \text{if } B'_\tau\left(\dot{\tau}^{(i)},\gamma\right) > 0 \tag{34.a}$$

$$\begin{cases} \acute{\tau}^{(i)} = \acute{\tau}^{(i-1)} \\ \grave{\tau}^{(i)} = \dot{\tau}^{(i)} \end{cases} \quad \text{if } B'_\tau\left(\dot{\tau}^{(i)},\gamma\right) < 0 \tag{34.b}$$

$$\acute{\tau}^{(i)} = \grave{\tau}^{(i)} = \dot{\tau}^{(i)} \quad \text{if } B'_\tau\left(\dot{\tau}^{(i)},\gamma\right) = 0 \tag{34.c}$$

$$\acute{\tau}^{(0)} = \tau_{\min} \tag{34.d}$$

$$\grave{\tau}^{(0)} = T \tag{34.e}$$

where, $\dot{\tau}^{(i)}$ is given by (34,f), as shown at the top of the this page, and i is the index of recursion time. $\tau_{\min}$ is given by

$$\tau_{\min} = \frac{\left(\mathrm{Q}^{-1}(p_{\mathrm{d}0})\right)^2}{f_{\mathrm{s}}}\left(\frac{1}{m} + \frac{2}{\gamma} + \frac{1}{\gamma^2}\right). \tag{34.g}$$

Proof: See Appendix B.

Therefore, the data rate loss $\Delta B_0(\gamma)$ can be upper bounded by $B_0(\gamma) - \tilde{B}_0(\gamma)$ and expressed as

$$\Delta B_0(\gamma) \le B_0(\gamma) - \tilde{B}_0(\gamma). \tag{35}$$

It is stated by the CLT, the distribution of the sum of any non-Gaussian distributed RVs can arbitrarily approach the Gaussian distribution, provided that the sizes of the samples are sufficiently large [13]. Accordingly, a proposition is as follows.

Proposition 3: The CDRL given by (32) will be arbitrarily small provided that the number of samples for detection is sufficiently large.

Proof: See Appendix C.

However, for the practical applications, the number of samples for detection will be finite. Therefore, formula (35) shows its applicability in estimating such a data rate loss of the CDRL.

V. APPROXIMATE DIRECT FORMULA OF OSD

A. THEORETICAL BASIS

Reference [1] has proved that $B(\tau,\gamma)$ of (25) (where $p_{\mathrm{f}}(\tau,\gamma) = \mathrm{Q}\left(\sqrt{2\gamma+1}\mathrm{Q}^{-1}(p_{\mathrm{d}0}) + \gamma\sqrt{f_{\mathrm{s}}\tau}\right)$) is concave w. r. t. τ. For the p_{f} of this paper in the new forms as (17), (22) and (24) give, does the concavity of the respective corresponding (25), (26) and (27) w. r. t. τ, still hold? We find it true. Therefore, another proposition is presented as follows.

Proposition 4: Let it be a condition that the signal of the licensed transmitter remains invariant while being sensed and propagates along a Nakagami-m fading channel prior to its arrival at the detector, where a CSCG distributed noise is added. Under such a condition, theorem 1, proposition 5 and 6 of [1] still hold for (25), (26) and (27).

Proof: See Appendix D.

It was mentioned that no solutions of $\tau_0(\gamma)$ of (28) and $\hat{\tau}_0(\gamma)$ of (29) w. r. t. γ exist in explicit closed forms. However, an implicit function mapping γ to τ_0 does exist [17]. Motivated by this, we consider piecewise fitting to be a good strategy for achieving an approximate direct formula of the OSD.

B. APPROXIMATE FORMULA BASED ON EXPONETIAL INTERPOLATION

For the sake of achieving the OSD via a direct formula instead of pure iteration, we propose a scheme that employs the exponential functions to piecewise approximate the exact OSD of (28). This direct formula is expressed in the form given by

$$\tilde{\tau}_0^i(\gamma) = \mu_i + \alpha_i e^{\varepsilon_i(\gamma-\beta_i)} \tag{36}$$

where i is the index of the ith piece, and μ_i, α_i, ε_i and β_i are the input parameters that can be calculated by solving a set of equations. See Appendix E for the acquisition of the above input parameters.

In Appendix E, you will observe that tiny iterations are still needed due to the need for the numerical calculations of $\tau_0(\gamma)$ at the starting points of all pieces. Let the γ values (as the horizontal axis of fig. 3 denotes) of the ends of all pieces be denoted by $\{r_i \mid i \in I\}$, where I is the set of indices of all pieces. Thus, $\{\mu_i, \alpha_i, \varepsilon_i, \beta_i\}$ will be determined by $\left\{r_i, \tau_0(r_i), \mathrm{d}\tilde{\tau}_0^i(r_i)/\mathrm{d}\gamma, r_{i+1}, \mathrm{d}\tilde{\tau}_0^i(r_{i+1})/\mathrm{d}\gamma\right\}$. In this sense, the scheme based on (36) falls under the category of interpolation. However, it is quite different from the popularly employed interpolation based on the Hermite spline [9], since our scheme requires the coincidences of the functions' values merely on the starting end of all pieces (i.e., $\tilde{\tau}_0^i(r_i) = \tau_0(r_i), \forall i \in I$). Faced by the derivation of an approximate PDF of $\tau_0(\gamma)$ based on $\tilde{\tau}_0^i(\gamma)$, the continuity of the PDF should be kept. In other words, the continuity of its 1st derivative $\mathrm{d}\tilde{\tau}_0^i(\gamma)/\mathrm{d}\gamma$ for all pieces as a whole

[1]The numeric calculation indicates that usually $(\mathrm{B}_0(\gamma) - B_0(\gamma))/B_0(\gamma) \le 10\%$ if $i \ge 2$. Thus, it does not need as many iterations to achieve a tight upper bound of $B_0(\gamma)$, i.e. $\mathrm{B}_0(\gamma)$.

must be guaranteed. This requirement is due to a fact that prior to getting the PDF of a function of a random variable, the 1st derivative of its inverse function has to be derived [13]. If the complexity or tractability of achieving such a PDF were not taken into account, undoubtedly the approaches based on polynomial interpolation (e.g., Hermite, B and rational splines) would be the better choices due to their fine performance [9]. Particularly, the cubic Hermite spline is particularly welcome since it features low order[2] polynomials meanwhile guarantees the curve's smoothness. Nevertheless, unfortunately all polynomial-based interpolation schemes are not applicable here for the four reasons as follows:

a) The complexity or intractability of the inverse function of $\tilde{\tau}_0^i(\gamma)$ if it is expressed by a polynomial,

b) The complexity of the 1st derivative of the inverse function of $\tilde{\tau}_0^i(\gamma)$ even if it is tractable,

c) The complexity or intractability of further derivations of other formulae of statistic characteristics (e.g., mathematical expectation and variance), and

d) The inevitability of operations of numeric iterations or matrix's inversions, which have superlinearly rising complexities with the increase of the number of pieces.

Consequently, the polynomial-based interpolants are not applicable to the context we are focusing on, since a highly mobile CR will surely be computational delay sensitive.

Therefore, as it is handled in Appendix E, it keeps the continuity of $\mathrm{d}\tilde{\tau}_0^i(\gamma)/\mathrm{d}\gamma$ at $\forall\gamma \in \{r_i \mid i \in I\}$ but it permits the slight discontinuity of $\tilde{\tau}_0^i(\gamma)$ thereon, as fig. 3 shows. In other words, if less continuity of $\tilde{\tau}_0^i(\gamma)$ can be swapped for more continuity of $\mathrm{d}\tilde{\tau}_0^i(\gamma)/\mathrm{d}\gamma$, $\forall i \in I$, it is worth being done. The reasons lie in a fact that the PDF of OSD (as (39) will show) is more sensitive to the latter than to the former, and our works for fig. 5 have experienced the same.

C. PDF OF OSD OVER A FADING VIA-TO-SENSE CHANNEL

As aforementioned, due to employing exponential splines $\left\{\tilde{\tau}_0^i(\gamma) \mid i \in I\right\}$ rather than polynomial-based ones, the inverse function of $\tilde{\tau}_0^i(\gamma)$ becomes smoothly derived. Therefore, based on (36), we derive it as

$$\tilde{\gamma}_i(\tau_0) = \beta_i + \frac{1}{\varepsilon_i}\ln\left(\frac{\tau_0 - \mu_i}{\alpha_i}\right). \tag{37}$$

Moreover, the logarithm function therein enables the extraordinarily easy derivation of its 1st derivative. The numerical result indicates that the curve of $\tau_0(\gamma)$ of (28) is concave-shaped as fig. 3 shows. Thus, the PDF of $\tilde{\tau}_0^i$ can be derived via the process as follows

$$\begin{aligned} & f_{\tilde{\tau}_0^i}(\tau) \\ &= \frac{\mathrm{d}F_{\tilde{\tau}_0^i}(\tau)}{\mathrm{d}\tau} = \frac{\mathrm{d}}{\mathrm{d}\tau}\int_{-\infty}^{\tau} f_{\tilde{\tau}_0^i}(t)\,\mathrm{d}t \\ &= \frac{\mathrm{d}}{\mathrm{d}\tau}\int_{-\infty}^{\tilde{\gamma}_l(\tau)} f_{\tilde{\gamma}_l}(\gamma)\,\mathrm{d}\gamma + \frac{\mathrm{d}}{\mathrm{d}\tau}\int_{\tilde{\gamma}_u(\tau)}^{\infty} f_{\tilde{\gamma}_u}(\gamma)\,\mathrm{d}\gamma \\ &= \frac{\mathrm{d}F_{\tilde{\gamma}_l}(\gamma)}{\mathrm{d}\gamma}\frac{\mathrm{d}\tilde{\gamma}_l}{\mathrm{d}\tau} - \frac{\mathrm{d}F_{\tilde{\gamma}_u}(\gamma)}{\mathrm{d}\gamma}\frac{\mathrm{d}\tilde{\gamma}_u}{\mathrm{d}\tau} = \frac{f_{\gamma_l}(\gamma)}{\varepsilon_l(\tau-\mu_l)} - \frac{f_{\gamma_u}(\gamma)}{\varepsilon_u(\tau-\mu_u)} \end{aligned} \tag{38}$$

where $F_X(\cdot)$ denotes the cumulative distribution function (CDF) of an RV X. ε_l & μ_l and ε_u & μ_u, denote ε_i & μ_i of (36), for which $\gamma \in \{\gamma \mid 0 \le \gamma \le \gamma_{\mathrm{p}}$ and $\gamma \in \{\gamma \mid \gamma_{\mathrm{p}} \le \gamma \le \infty$, respectively, where $\gamma_{\mathrm{p}} = \arg\max_{0\le\gamma\le\infty}\tau_0(\gamma)$.

As (4) shows, $f_{\gamma_l}(\gamma)$ and $f_{\gamma_u}(\gamma)$ within (38) follow a gamma distribution. Replacing them with (4) leads to an approximate PDF of the OSD over a Nakagami-Gamma shadowed fading via-to-sense channel. Notice that (38) is conditioned on M and $\bar{\gamma}$. On this account, we reformulate it into a conditional PDF as

$$\begin{aligned} & f_{\tilde{\tau}_0}(\tau \mid M, \bar{\gamma}) \\ &= \frac{(\tilde{\gamma}_l(\tau))^{M-1} e^{-\tilde{\gamma}_l(\tau)/\bar{\gamma}}}{\Gamma(M)\bar{\gamma}^M\varepsilon_l(\tau-\mu_l)} - \frac{(\tilde{\gamma}_u(\tau))^{M-1} e^{-\tilde{\gamma}_u(\tau)/\bar{\gamma}}}{\Gamma(M)\bar{\gamma}^M\varepsilon_u(\tau-\mu_u)} \\ &= \frac{\left[\beta_l + \frac{1}{\varepsilon_l}\ln\left(\frac{\tau-\mu_l}{\alpha_l}\right)\right]^{M-1}\left[\exp\left(\frac{\beta_l}{\bar{\gamma}}\right) + \left(\frac{\tau-\mu_l}{\alpha_l}\right)^{(1/\bar{\gamma}\varepsilon_l)}\right]}{\Gamma(M)\bar{\gamma}^M\varepsilon_l(\tau-\mu_l)} \\ &\quad - \frac{\left[\beta_u + \frac{1}{\varepsilon_u}\ln\left(\frac{\tau-\mu_u}{\alpha_u}\right)\right]^{M-1}\left[\exp\left(\frac{\beta_u}{\bar{\gamma}}\right) + \left(\frac{\tau-\mu_u}{\alpha_u}\right)^{(1/\bar{\gamma}\varepsilon_u)}\right]}{\Gamma(M)\bar{\gamma}^M\varepsilon_u(\tau-\mu_u)} \end{aligned} \tag{39.a}$$

where τ determines which two pieces among all cover it, as fig. 3 shows. Let the smaller and larger i-valued pieces be indexed by l and u, respectively, they are given by

$$\begin{cases} l = \min\left\{i \mid \tilde{\tau}_0^i = \tau, i \in I\right\} \\ u = \max\left\{i \mid \tilde{\tau}_0^i = \tau, i \in I\right\}. \end{cases} \tag{39.b}$$

Formula (39) is just the targeted PDF of the OSD, which may be significantly interesting to those who study the CR system's cross-layer problems. Let us give an example. The frame alignment delay is a key contributor to the user-plane latency budget, which additionally includes the queuing, transmission and processing delays [25], [26]. Such a frame alignment can be illustrated by fig. 1. Therein, T is the frame period that is usually configured to be identical to the transmission time interval (TTI) [26]. τ_0 and $T - \tau_0$ are the sensing and data transmission durations, respectively. a_k and $\mathrm{a'}_k$ are the upper-layer data's two possible arrival instants, while e_k and e_{k+1} are its entrance instant in the kth frame and

[2]Interpolation using polynomials of degrees higher than 3 is very likely to suffer from Runge's phenomenon (i.e. oscillation at the edges of interval). Thus, the cubic type is usually considered to be the most effective polynomial-based interpolant [9]. Moreover, Galois proved that a polynomial with its order higher than 4 is not ensured to get the real root [18], and thus its inverse function may also be unachievable.

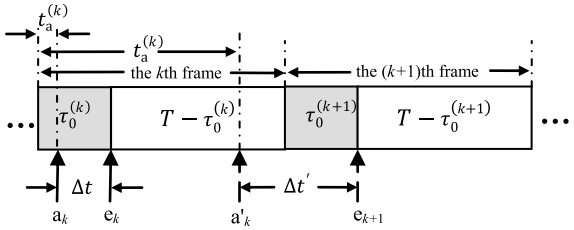

FIGURE 1. Constituent Time Slots of a Frame Period and the Frame Alignment Mechanism of the CR system. Therein, T is the frame period, τ_0 and $T-\tau_0$ are for sensing and data transmission, respectively; a_k and a'_k are the upper-layer data's two possible arrival instants while e_k and e_{k+1} are its entrance instant in the kth frame and its next frame, respectively. There are two cases for the current data to enter the radio frame. In the first case, it arrives at a_k, and enters the current frame at e_k; In the second case, it arrives at the instant of a'_k, then no chance for it to enter the current frame, so it has to wait till the e_{k+1} arrives.

the next frame, respectively. Two random events will possibly occur for the arriving data's entrance to the radio frame. In the first case, the data packet will arrive at the buffer output in the instant of a_k with a time span of $t_a^{(k)}$, $0 \le t_a^{(k)} \le \tau_0$ to the starting instant of the frame. It will wait for a shorter duration to come into the current radio frame at e_k. In the second case, the data packet arrives in the instant of a'_k with $t_a^{(k)}$ranging within $\tau_0 \le t_a^{(k)} \le T$. Then, it has no chance within the current frame for its entrance, and it has to wait for a longer duration until the next frame's entrance e_{k+1} arrives.

The $t_a^{(k)}$ of fig. 1 is usually uniformly distributed within the frame period [25]. Without the loss of generality, let t_a as a RV represent $t_a^{(k)}$, $\forall k$. Thus, the PDF of t_a is given by

$$f_{t_a} = 1/T, \quad 0 \le t_a \le T \tag{40.a}$$

Let the frame alignment delay of the CR system be denoted as d_{fa} and just be the Δt or $\Delta t'$ in fig. 1. Obviously, we have $d_{fa} = \tau_0 - t_a$ with the probability of τ_0/T, and $d_{fa} = T - t_a + \tau_0$ with probability of $(T-\tau_0)/T$, respectively. Therefore, the PDF of the frame alignment delay of a CR system denoted as $f_{d_{fa}}$ is derivable based on the law of PDF of sum of RVs [13]. It is given by

$$f_{d_{fa}}(x) = \left(f_{\tilde{\tau}_0} \otimes f_{(-t_a)}\right)\frac{\tau_0}{T} + \left(f_{\tilde{\tau}_0} \otimes f_{(T-t_a)}\right)\frac{T-\tau_0}{T} \tag{40.b}$$

where $f_{\tilde{\tau}_0}$, $f_{(-t_a)}$ and $f_{(T-t_a)}$ are given by (39) and (40.a), respectively, while the sign $\otimes$ is a convolution operator.

Accordingly, furthermore, the mean delay of the frame alignment of a CR system denoted by $\bar{d}_{fa}$ is also achievable. It is given by

$$\bar{d}_{fa} = \int_0^T x f_{d_{fa}}(x)\,dx \tag{40.c}$$

Formulas (40.c) and (40.b) indicate that such a PDF of the OSD of (39) is of significant importance to a CR system's frame alignment and other cross-layer operations.

Moreover, notice that formula (39) depends on M and $\bar{\gamma}$ and still keeps an exponential form, which enables the particularly troubleless integral operation of its product with an exponential-formed function (e.g., (4)). Consequently, we made little effort to derive an approximate formula of mean OSD as

$$\begin{aligned}\mathbb{t}_0(M,\bar{\gamma}) &\cong \sum_{i=1}^{N}\int_{r_i}^{r_{i+1}} \tilde{\tau}_0^i(y) f_\gamma(y|\bar{\gamma})\,dy \\ &= \sum_{i=1}^{N}\left[\Im_\tau^i(r_{i+1}) - \Im_\tau^i(r_i)\right]\end{aligned} \tag{41.a}$$

where $f_\gamma(y|\bar{\gamma})$ is given by (4) and r_i is the value of γ at the starting end of the ith piece. $\Im_\tau^i(\gamma)$ is the result of $\int \tilde{\tau}_0^i(y) f_\gamma(y|\bar{\gamma})\,dy$ and is given by

$$\Im_\tau^i(\gamma) = -\frac{(\gamma/\bar{\gamma})^M}{\Gamma(M)}\left(\frac{\alpha_i e^{-\beta_i\varepsilon_i}\Gamma(M,\gamma/\bar{\gamma}-\varepsilon_i\gamma)}{(\gamma/\bar{\gamma}-\varepsilon_i\gamma)^M} + \frac{\mu_i\Gamma(M,\gamma/\bar{\gamma})}{(\gamma/\bar{\gamma})^M}\right) \tag{41.b}$$

In (41.b), $\bar{\gamma}$ and M (which was explained for (4)) explicitly reflect the status of shadow fading, while μ_i, α_i, ε_i and β_i defined for (36) implicitly reflect the status of Nakagami-m fading as fig. 3 demonstrates. Such implicity is due to the unachievability of an explicit formula mapping τ_0 to m.

D. ERGODIC-SENSING CHANNEL CAPACITY

Similar to using (36) to fit (28), $B_0(\gamma)$ of (30) can also be approximated by piecewise exponential functions. The latter is found more easily handled, with three pieces to do it well. It is

$$\tilde{B}_0^j(\gamma) = u_j + v_j e^{k_j(\gamma - w_j)}, \quad j = 1,2,3. \tag{42}$$

Along the same way as Appendix E addresses (36), all input parameters of (42) are acquirable.

Since formula (42) is still of an exponential form, the inverse functions of $\tilde{B}_0^j(\gamma), j = 1,2,3$ are also quite easily derived as

$$\tilde{\gamma}_j(B_0) = w_j + \frac{1}{k_j}\ln\left(\frac{B_0 - u_j}{v_j}\right). \tag{43}$$

We find that $\tilde{B}_0^j(\gamma)$ increases monotonically with the increase of γ. Therefore, by directly invoking the related formula of the PDF of a function of a random variable [13], the PDF of $B_0(\gamma)$can be smoothly derived still in a piecewise exponential form given by

$$f_{\tilde{B}_0^j}(B\,|\,M,\bar{\gamma}) = \frac{\left(\tilde{\gamma}_j(B)\right)^{M-1}}{\bar{\gamma}^M\Gamma(M)\,|k_i(B-u_i)|}e^{-\frac{\tilde{\gamma}_j(B)}{\bar{\gamma}}} \tag{44}$$

where $\tilde{\gamma}_j(B_0)$ is given by (43).

In some cases, the data rate performance of a CR system over a longer term must be evaluated, rendering such a definition quite necessary as follows.

Definition 1: The *Normalized Ergodic Sensing Capacity* (*NESC*) is defined as the statistically averaged MADR of (30)

for a CR system whose via-to-sense channel experiences a long term fading. It is given by

$$\mathbb{B}_0(M,\bar{\gamma}) = \int_0^{\infty} B_0(y) f_{\gamma}(y|\bar{\gamma})\,\mathrm{d}y \tag{45}$$

where $f_{\gamma}(y|\bar{\gamma})$ denotes the PDF of γ conditioned on $\bar{\gamma}$, which is given by (4). The replacement of the integrand with the product of (42) and (4) yields

$$\mathbb{B}_0(M,\bar{\gamma}) \cong \sum\nolimits_j \left[\mathcal{T}_B^j\left(r_{j+1}\right) - \mathcal{T}_B^j\left(r_j\right)\right] \tag{46}$$

where $\mathcal{T}_B^j(\gamma), j = 1,2,3$ is the indefinite integral of $B_0(\gamma) f_{\gamma}(y|\bar{\gamma})$ along the jth piece. It is given by

$$\mathcal{T}_B^j(\gamma) = -\frac{u_i \Gamma(M, \gamma/\bar{\gamma} - k_i\gamma)}{\Gamma(M)} - \frac{\gamma^M v_i e^{-k_i w_i} \Gamma(M, \gamma/\bar{\gamma} - k_i\gamma)}{\bar{\gamma}^M \Gamma(M)(\gamma/\bar{\gamma} - k_i\gamma)^M}. \tag{47}$$

So far, a set of formulae for approximately evaluating some sensing-related statistic information (i.e., the PDFs of the OSD and MADR and their statistic mean values), has been achieved. Then, one may raise such a question as follows.

Under the context of a CR or its sensed objects at high mobility, why is it so desirable to quickly acquire the OSD, the MADR, and their related statistic information? The reasons are as follows.

It can been seen from (30) and the related (17), the B_0 of MADR depends on γ and the other three parameters of T, f_s and p_{d0}. Obviously, the OSD depends on γ. At high mobility, in addition to the rapid fluctuation of γ, the latter three are also quite likely to vary quickly. Hence, they need to be timely updated to follow the rapid variation of the radio environment described as follows.

a) Since a wireless device usually moves at a varying velocity, surely its channel coherence time will vary correspondingly. Consequently, the temporal interval of channel estimation should be timely updated to adapt to the variation of its movement velocity. Therefore, T (the period of a data frame) should also be swiftly adjusted for a higher efficiency of QoS management to be achieved (e.g., the maximal traffic [11], or the triple trade-off of TTI, queuing delay and spectrum efficiency [25]).

b) The bandwidth being sensed may also vary frequently since the variant licensed signals that may carry different services are ready for the CR to detect them. For example, the video service usually needs a much wider bandwidth than the audio one. Therefore, following Nyquist's sampling theorem, f_s should also be flexible rather than fixed in order to timely adapt to the variations of sensed bandwidths.

c) Different licensed services require different QoS, making their requirements on the symbol error rate (SER) quite different [11]. For example, the audio service usually requires less SER than a text file. Therefore, as a licensed service, it requires much less p_{d0} of the CRs that intend to access in. Thus, to adapt to the variant licensed system with different sensitivities to the interference, p_{d0} should also be timely reconfigured to minimize the network latency.

Overall, we are facing the wireless environment as follows. All aforementioned parameters are varying rapidly while multiple licensed bands (e.g., the subchannels of an Orthogonal Frequency Division Multiple Access (OFDMA) system) are alternating quickly between business and idleness. Under such a context, it is of significant importance for a CR system to quickly learn the probability distribution of the OSD and the MADR of each band that certain devices intend to access. Only with awareness of the aforementioned statistical information are the relevant QoS managements (e.g., the call admission control (CAC) [11] and frame alignment [25] illustrated by fig. 1) capable of being performed more efficiently [11], [26].

E. COMPLEXITY ANALYSIS OF EI vs. HI

For high mobility, lower complexity should be preferred to higher accuracy for an algorithm. Therefore, peer-to-peer comparisons will be done on the complexities of the above formulae, which are based on EI or HI that is supposed to be applied as EI's alternative.

1) FORMULA OF THE OSD OF (36) AND THE MADR OF (42)

Formulae (36) and (42) in their current forms involve the simplest operations such as addition, subtraction and multiplication. Meanwhile, the exponential functions therein can be easily transformed into the above operations by series expansion.

Nevertheless, if HI is applied here, a set of linear equations have to be solved, which fall into more difficult operations such as matrix inversions or numerical iterations. As a result, the incurred operations will considerably exceed those needed by the EI scheme, just as Appendix E reveals.

As fig. 3 shows, it does not need so many pieces to achieve an acceptable precision if the interpolating points are properly located. The reason that we analyse may lie in a fact that the objective curves of eq. (28) and (30) are inherently exponential-alike.

2) FORMULA OF OSD PDF OF (39) AND THAT OF MADR PDF OF (44)

The form of the OSD PDF of (39) and the MADR PDF of (44) would become significantly different if HI were applied as an alternative. Suppose that HI (say a cubic Hermite spline) is applied to their corresponding derivation procedures. It will incur two troublesome problems as follows. i) Although deriving the inverse function of a polynomial of degree 3 (i.e., cubic) is possible if employing the Cardano formula [21], it is still not a simple form. ii) Even if the derivation of the inverse function is tractable, the resultant formulae will still be of much higher complexity than (37) and (43), which are simply logarithm forms. More beneficially, the logarithm form (as is well-known) has a considerably simpler form of its 1st derivative that can be achieved with little effort.

3) FORMULA OF THE OSD'S MATHEMATICAL EXPECTATION OF (41.a) AND THAT OF THE MADR'S OF (46)

Due to high mobility, it is quite likely that we encounter a demanding case where operation speed is almost always preferred to precision. In such a context, if the HI scheme is chosen instead of the EI scheme, the polynomial of degree 2 has to be employed based on the consideration that it has the lowest complexity as a spline function. Even if it was done in this way, the formula (41.b) (which is the essence of formula (41.a)) would turn to

$$\Im_{\tau}^{i}(\gamma) = \frac{1}{\Gamma(M)} \sum\nolimits_{n=0}^{2} p_{i,n} \bar{\gamma}^{n} \Gamma\left(M+n, \frac{\gamma}{\bar{\gamma}}\right) \quad (48)$$

where $p_{i,n}$ denotes the coefficient of the nth power term of the polynomial fitting the ith piece. It shows that even if it is purposely done in such a way to make HI as operation-reduced as possible, the number of terms of (48) still reach 3 with a 50% increase over that of (41.b) resulting from EI.

For formula (46) (namely, NESC), its complexity analysis will be in the same way if done.

So far, overall, it can be concluded that the EI scheme is a more operations-saving approach than the HI scheme to achieve the above information, the awareness of which will lead a CR network to have more efficient traffic.

VI. SIMULATION RESULTS

With the aim to verify the theoretical results in the preceding sections, we place them in a scenario that a CR system at high mobility is sensing a licensed frequency band via a Nakagami-Gamma shadowed fading channel. The Nakagami fading parameter m is configured to be 1/2, 1 and 3, which represent three typical fadings (i.e., the single-side Gaussian, Rayleigh and Rician fading), respectively. The shape parameter M of the Gamma distribution that characterizes the shadow fading will be configured to be the same as m. All licensed bands are of the OFDMA system, which occupies a bandwidth of 10 MHz denoted BW and is equally divided into 100 subchannels. Therefore, each subchannel bandwidth denoted bw equals 100KHz. The licensed system's maximal tolerable interference requires p_{d0} to be 0.90 or 0.99.

To testify the applicability of the CLT to the context described as above, we compare the exact MADR (30) and its CLT-resultant counterpart (31). Suppose that all subchannels experience the independently identically distributed (i.i.d.) fadings, and, without the loss of generality, we select one of them to be analysed. Here, the T (the duration of a data frame) is configured to be as small as 2 ms, which implies that high mobility exists.

Fig. 2 shows that the exact (ideal) and CLT-resultant (non-ideal and approximate) MADRs (as defined by (30) and (31), respectively) are quite close under the parameters specified below the figure. It is shown that even if T is configured to be as small as 2 ms, the data rate losses are expected to be no more than 0.05, 0.03 and 0.02 for $m = 1/2$, 1 and 3, respectively. It should be noted that this value of 2 ms has reached the lower bound of the data frame period specified by

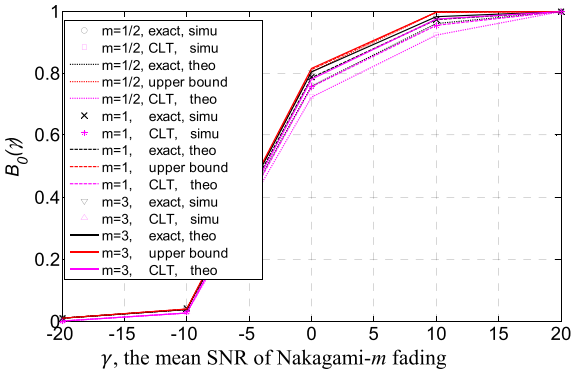

FIGURE 2. Normalized maximal achievable data rate vs. the mean SNR of Nakagami-m fading with various fading parameters m. [$p_{\mathrm{d0}} = 0.99$, $bw = 100$KHz, $T = 2$ ms, and i of (34) configured to be 3].

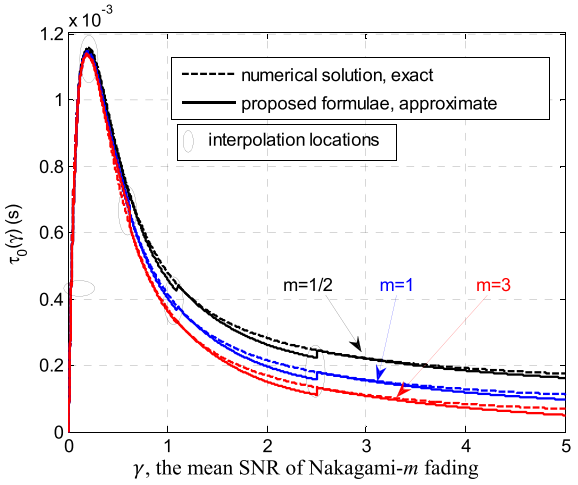

FIGURE 3. Optimal sensing duration vs. the mean SNR of Nakagami-m fading with various fading parameters m. ($p_{\mathrm{d0}} = 0.99$, bw=100KHz, and $T = 2$ ms).

IEEE 802.16e [19]. This justifies the applicability of the CLT under the specified mobility context. Moreover, it shows that the upper bound of the data rate (as (33) presents) can achieve satisfactory tightness so long as i of (34) is configured to be no less than 3. Thus, we can argue that this analysis provides us a tool to quickly estimate the MADR and the resultant data rate loss due to CLT.

For a precision evaluation of formula (36) (as Fig. 3 shows), we compare the OSD results by directly invoking (36) with those of (28), which are obtained via numerical iteration and are regarded as the exact ones. The numerical iteration approach is based on the method of Golden Section (GS) [20]. It shows that it is not a bad fit for the two results' alignment within the whole range of each piece, except for in the vicinity of the boundaries of adjacent pieces where a slight error still occurs. Such an error is due to (as it is explained in subsection V.B) the absence of the constraint of the function values' coincidence on both ending points of each piece.

For an algorithm applicable to mobility, the operation complexity usually becomes an equally or even more important performance. Therefore, we conduct an evaluation of

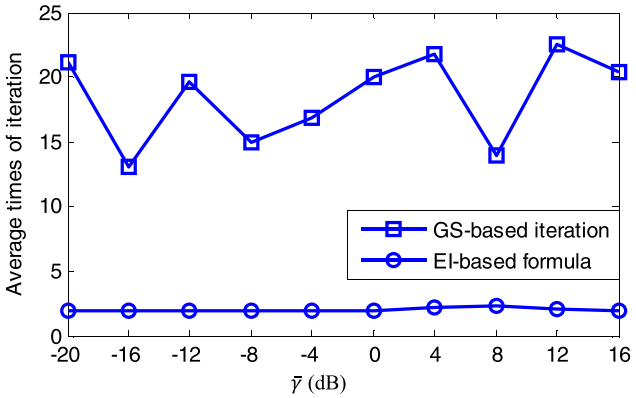

FIGURE 4. Average times of iteration for calculating OSD under variant $\bar{\gamma}$, i.e., the mean SNRs of shadow fading ($M = 1$, $m = 1$, $p_{d0} = 0.99$, bw=100KHz, $T = 2$ ms, and 100 samples of γ for each $\bar{\gamma}$).

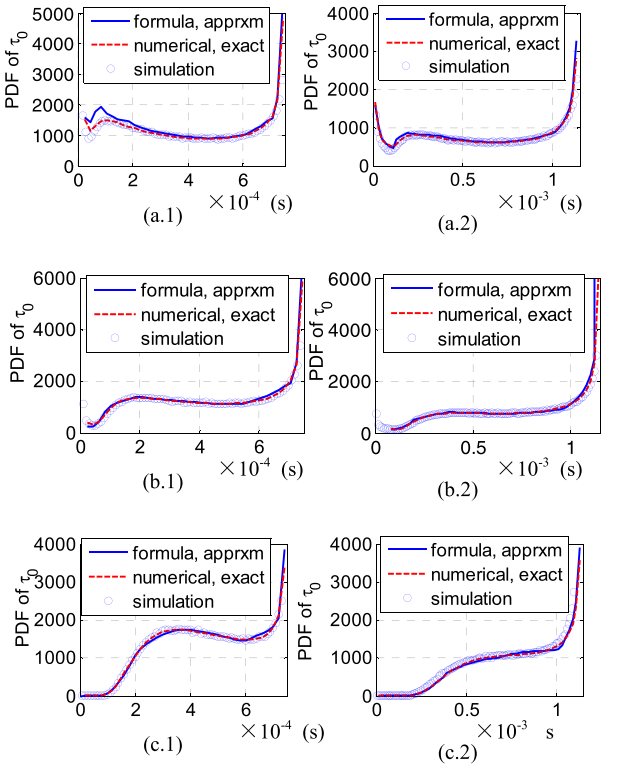

FIGURE 5. PDF of the OSD over a Nakagami-Gamma shadowed fading via-to-sense channel with different M and p_{d0}. (a.1) τ_0 ($M = 1/2$, $p_{d0} = 0.90$). (a.2) τ_0 ($M = 1/2$, $p_{d0} = 0.99$). (b.1) τ_0 ($M = 1$, $p_{d0} = 0.90$). (b.2) τ_0 ($M = 1$, $p_{d0} = 0.99$). (c.1) τ_0 ($M = 3$, $p_{d0} = 0.90$). (c.2) τ_0 ($M = 3$, $p_{d0} = 0.99$).

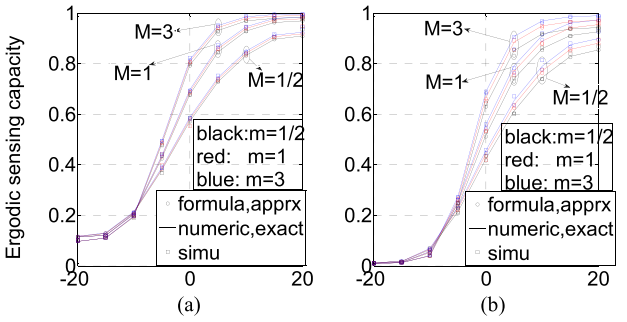

FIGURE 6. Normalized ergodic-sensing capacity vs. mean SNR of shadow fading under different Pd0 and fading parameters (BW = 10MHz, $T = 2$ ms, and 100 samples of γ for each $\bar{\gamma}$). (a) $\bar{\gamma}$ (dB) ($p_{d0} = 0.90$). (b) $\bar{\gamma}$ (dB) ($p_{d0} = 0.99$).

complexity of the EI-based formula (36) by comparing its computational effort with that of an iteration scheme based on Golden Section. We generate 10 sets of Gamma distributed samples of γ with unified sizes of 100 but different mean values (i.e., $\bar{\gamma}$ for each set). As mentioned, they are regarded as the 10 sets of alternatives of logarithm-Gaussian distributed SNRs reflecting different shadow fadings. As Appendix E shows, a small number of iterations is still needed by executing (28) to achieve (36) since the exact OSD values at the boundaries of adjacent pieces (as fig. 3 shows) have to be calculated prior. Therefore, we let the number of iterations resulting from formula (36) be a contrast with that resulting from applying the GS to (28) based on the one-by-one sample of γ. Such a way for comparison is based on the consideration that each set of γ samples are regarded as a provider of a task that calculates all OSDs either by invoking formula (36) or by purely applying the iteration approach (e.g., based on GS). Thus, fig. 4 shows the average number of iterations needed by per γ sample's handling (i.e., per sensing operation) for the ten sets of samples. It indicates that invoking formula (36) to solve problem (28) over a Rayleigh-Gamma shadowed fading channel will save approximately 90% of the iterations needed by the GS-based approach.

Fig. 3 and fig. 4 jointly justify formula (36) to be an effective tool to achieve the OSD for those CR systems that are highly sensitive to computation delay due to their high mobility.

It has been stated that the PDF of the OSD can be approximately expressed by (39), where it depends implicitly (via α, β, μ and ε) on m and explicitly on M. Therefore, the PDFs for a fixed m under different p_{d0} and M that reflect some typical shadow fadings are illustrated in fig. 5. It can be seen that the results based on formula (39), the numerical iteration scheme based on the GS approach (i.e., resulting from numeric solution of $\tau_0(\gamma)$, as fig. 3 shows) and Monte Carlo simulation coincide well. Fig. 5 also reveals that a higher p_{d0} leads to a wider OSD range. Such a phenomenon confirms a fact that the increase of p_{d0} will statistically need more time for sensing to keep a higher p_{d0}. It is also shown that the rise of M statistically increases the OSD. The reason of this dependence may be hidden behind the fact that the rise of M renders γ more Rician or statistically more concentrated around $\bar{\gamma}$ of 0.5, which occurs to approach the γ value corresponding to the peak of $\tau_0(\gamma)$, as fig. 3 shows.

Fig. 6 shows the normalized ergodic-sensing capacity as defined by (45) for a wider bandwidth having 10 i.i.d. subchannels as fig. 3 demonstrated. It varies with different mean SNR $\bar{\gamma}$ under different m, M and p_{d0}. It reveals that this kind of channel capacity decreases with the increase of p_{d0},

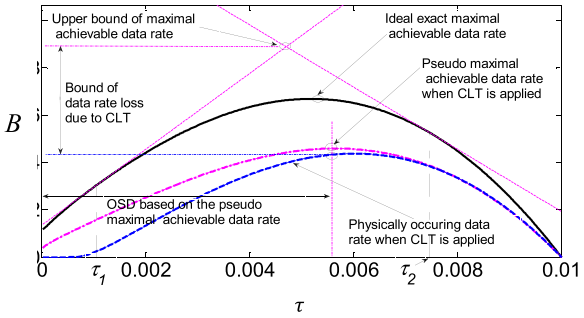

FIGURE 7. **Illustration of the bound of the data rate loss due to the CLT. [Therein τ_1 and τ_2 are $\dot{\tau}$ and $\grave{\tau}$ of (33.a), respectively].**

and a lower $\bar{\gamma}$ results in a more significant decrease. This confirms the fact that the protection of the licensed system's communication damages the cognitive one to a certain extent. Fig. 6 also shows that the increase of M may increase capacity, and this rise becomes highlighted within a certain range centred at approximately 5 dB. The cause of the occurrence is that the corresponding range of $\bar{\gamma}$ occurs to fall in the sharply rising region of the CDF of the Gamma distribution. However, the increase of m can only slightly raise the channel capacity. The higher that the p_{d0} is configured, the more significant such an increase gets. The former phenomenon is due to the fact that M is more dominant than m for a Nakagami-Gamma fading channel, while the latter is due to $\Gamma_0^{-1}\left(K\xi\left(m,\gamma\right),p_{\mathrm{d0}}\right)$ within ε_0 of (14), since $\Gamma_0^{-1}\left(a,z\right)$ as a generic form falls sharply as $z\to 1$ if $a\gg 1$ [23].

VII. CONCLUSIONS

For a CR network, the optimal sensing duration (OSD) enables the maximization of data throughput. In that effort, the CLT is widely applied, which can significantly simplify the related analyses and operations but results in the side effect of the loss of data rate. For the sake of estimating such a loss, an approach to achieve a tight upper bound of the maximal achievable data rate (MADR) over Nakagami-m fading via-to-sense channel is proposed. Moreover, for a CR system in a mobile environment, a direct formula of the OSD will be considerably desired since such a formula is more capable than an iteration scheme of keeping up with the rapid variation of channel and the availability of spectrum holes. To meet such a need, an approach based on exponential interpolation is proposed. Such an approach is confirmed to be quite beneficial when dealing with the Nakagami-Gamma shadowed fading via-to-sense channel, since it renders the subsequent derivations of the PDF of the OSD, the ergodic-sensing capacity and other related statistical informations significantly tractable. Of course, quick awareness of those informations via such an approach can help the CR systems to more efficiently perform their QoS management. Furthermore, this study indicates that the exponential-formed function will likely be a better choice than any other forms if one intends to approximate a function concerning a certain type of fading based on Gamma families (e.g., Nakagami-m including Rayleigh, Rician, etc.).

APPENDIX A
THE PROOF OF PROPOSITION 1

Proof: Under hypothesis $\mathcal{H}_1$, based on (2), we have

$$|y\left(k\right)|^2=\left(s\left(k\right)+z\left(k\right)\right)\left(s^*\left(k\right)+z^*\left(k\right)\right) \tag{A.1}$$

Due to the independence between $s\left(k\right)$ and $z\left(k\right)$, the expansion of (A.1) yields

$$\mu_{\mathcal{H}_1}=E\left(|s\left(k\right)+z\left(k\right)|^2\right)=\sigma_z^2+\sigma_s^2=(1+\gamma)\sigma_z^2 \tag{A.2}$$

It is indicated in (3) that $\gamma\sim \mathrm{Ga}(m,\gamma/m)$ means that $|s\left(k\right)|^2\sim \mathrm{Ga}(m,\sigma_S^2/m)$ since $\sigma_z^2$is assumed to be a constant here. Therefore, the mean and variance of $|s\left(k\right)|^2$ are derived based on a related formulae for the Gamma distribution [13] given by

$$E\left(|s\left(k\right)|^2\right)=m\frac{\sigma_S^2}{m}=\sigma_S^2 \tag{A.3}$$

$$D(|s\left(k\right)|^2)=m(\frac{\sigma_S^2}{m})^2=\frac{\sigma_S^4}{m} \tag{A.4}$$

respectively. Thus, based on a property of variance [13], the $\mathrm{E}\left(|s\left(n\right)|^4\right)$ is accordingly derived to be

$$\mathrm{E}\left(|s\left(k\right)|^4\right)=D(|s\left(k\right)|^2)+E^2\left(|s\left(k\right)|^2\right)=(1+\frac{1}{m})\sigma_S^4 \tag{A.5}$$

For any CSCG distributed noise sample $z\left(k\right)$, $\mathrm{E}\left(|z\left(k\right)|^4\right)=2\sigma_z^4$ [1]. Its and (A.5)'s substitution into (8) of [1] yields

$$\begin{aligned}\sigma_{\mathcal{H}_1}^2&=\frac{1}{K}[E\left(|s\left(k\right)|^4\right)+E\left(|z\left(k\right)|^4\right)-\left(\sigma_S^2-\sigma_z^2\right)^2]\\&=\frac{\sigma_z^4}{K}\left[\frac{1}{m}\gamma^2+2\gamma+1\right]\end{aligned} \tag{A.6}$$

Since $y\left(k\right)$ of (2) is the sum of two RVs, $s\left(k\right)$ and $z\left(k\right)$ are both CSCG distributed with $\mathrm{CN}\left(0,\sigma_s^2\right)$ and $\mathrm{CN}\left(0,\sigma_z^2\right)$, respectively. Therefore, $y\sim CN\left(0,\sigma_S^2+\sigma_z^2\right)$. Accordingly, $\mathrm{T}\left(y|\mathcal{H}_1\right)$ of (7) can be treated as the sum of multiple squared amplitudes of CSCG-distributed RVs. Therefore, $T\left(y|H_1\right)$ of (7) is Gamma distributed and denoted as $\mathrm{Ga}(\kappa,\theta)$, where κ and θ are derivable based on the property of the Gamma distribution [13] as

$$\theta=\frac{\sigma_{\mathcal{H}_1}^2}{\mu_{\mathcal{H}_1}}=\frac{\sigma_z^2}{K}\cdot\frac{\gamma^2/m+2\gamma+1}{1+\gamma} \tag{A.7}$$

$$\kappa=\frac{\mu_{\mathcal{H}_1}}{\theta}=\frac{K(1+\gamma)^2}{\gamma^2/m+2\gamma+1} \tag{A.8}$$

APPENDIX B
THE PROOF OF PROPOSITION 2

Proof: First, let us prove the (33.c) to be true as follows. The 1st derivative of p_{f} of (16) w.r.t. τ is given by

$$p_{\mathrm{f}}'\left(\tau\right)=\frac{\Gamma_\tau'\left(K,K\varepsilon_0/\sigma_z^2\right)\Gamma\left(K\right)-\Gamma\left(K,K\varepsilon_0/\sigma_z^2\right)\Gamma_\tau'\left(K\right)}{\Gamma^2\left(K\right)} \tag{B.1}$$

where

$$\begin{aligned}&\Gamma'_\tau(K)\\&=\Gamma'_K K'_\tau=f_s\int_0^\infty \ln(\zeta)\,\zeta^{K-1}e^{-\zeta}\mathrm{d}\zeta;\qquad\text{(B.2)}\\&\Gamma'_\tau\left(K,K\varepsilon_0/\sigma_z^2\right)\\&=\Gamma'_K\left(K,K\varepsilon_0(K)/\sigma_z^2\right)K'_\tau\cdots\\&=f_s\left(\frac{\partial\Gamma\left(K,K\varepsilon_0/\sigma_z^2\right)}{\partial K}+\frac{\partial\Gamma\left(K,K\varepsilon_0/\sigma_z^2\right)}{\partial\left(K\varepsilon_0/\sigma_z^2\right)}\frac{\mathrm{d}\left(K\varepsilon_0/\sigma_z^2\right)}{\mathrm{d}K}\right).\qquad\text{(B.3.1)}\end{aligned}$$

Eq. (14) leads to $K\varepsilon_0/\sigma_z^2=((1+\gamma)/\xi)\,\Gamma_0^{-1}(\xi K,p_{\mathrm{d}0})$, so

$$\frac{\mathrm{d}\left(K\varepsilon_0/\sigma_z^2\right)}{\mathrm{d}K}=(1+\gamma)\frac{\mathrm{d}\left(\Gamma_0^{-1}(\xi K,p_{\mathrm{d}0})\right)}{\mathrm{d}(\xi K)};\qquad\text{(B.3.2)}$$

Based on the formula of the derivative of inverse regularized incomplete Gamma function w.r.t. the shape parameter [23], we have

$$\begin{aligned}\mathrm{d}\left(\Gamma_0^{-1}(\xi K,p_{\mathrm{d}0})\right)/\mathrm{d}(\xi K)=&\cdots\\&e^w w^{1-\xi K}[w^{\xi K}\Gamma^2(\xi K)\cdots\\&\cdot{}_2\tilde{F}_2(\xi K,\xi K;\xi K+1,\xi K+1;-w)\cdots\\&+(p_{\mathrm{d}0}-1)\,\Gamma(\xi K)\log(w)\cdots\\&+(\Gamma(\xi K)-\Gamma(\xi K,w))\,\psi(\xi K)]\qquad\text{(B.3.3)}\end{aligned}$$

where $w=\Gamma_0^{-1}(\xi K,p_{\mathrm{d}0})$, and ${}_2\tilde{F}_2(;;)$ is the hypergeometric function [24]. Based on the formula of the derivative of the incomplete Gamma function w.r.t. its shape parameter [23], we have

$$\begin{aligned}\frac{\partial\Gamma\left(K,K\varepsilon_0/\sigma_z^2\right)}{\partial K}=&\cdots\\&\Gamma^2(K)\left(K\varepsilon_0/\sigma_z^2\right)^K\cdots\\&\cdot{}_2\tilde{F}_2\left(K,K;K+1,K+1;-K\varepsilon_0/\sigma_z^2\right)\cdots\\&-\Gamma\left(K,0,\frac{K\varepsilon_0}{\sigma_z^2}\right)\log\left(\frac{K\varepsilon_0}{\sigma_z^2}\right)+\Gamma(K)\,\psi(K)\qquad\text{(B.3.4)}\end{aligned}$$

where $\psi(\cdot)$ is the Psi function [24]. Based on that, w.r.t its lower limit of integral [23], we have

$$\frac{\partial\Gamma\left(K,K\varepsilon_0/\sigma_z^2\right)}{\partial\left(K\varepsilon_0/\sigma_z^2\right)}=-\left(\frac{K\varepsilon_0}{\sigma_z^2}\right)^{K-1}e^{-\frac{K\varepsilon_0}{\sigma_z^2}}\qquad\text{(B.3.5)}$$

The substitutions of (B.3.2) [thereof a corresponding part replaced with (B.3.3)], (B.3.4) and (B.3.5) into (B.3.1) render it solvable. Then, the substitutions of (B.2) and (B.3.1) into (B.1) lead to a solvable $p'_{\mathrm{f}}(\tau)$ in an explicit form, just as (33.c) shows.

Second, we prove that $B_0(\gamma)\le\mathcal{B}_0(\gamma)$ and $\mathcal{B}_0(\gamma)\to B_0(\gamma)$ with $i\to\infty$ where i is that within (34), as follows.

Based on proposition 4, just as the context specified by [1], the $B(\tau,\gamma)$ of (25) is also concave if $p_{\mathrm{f}}(\tau)\le 0.5$ and it has a unique maximum w. r. t. τ. Since $p_{\mathrm{f}}\le\hat{p}_{\mathrm{f}}$, $\hat{p}_{\mathrm{f}}(\tau)=0$ yields a solution of $\tau_{\min}$ that also satisfies $p_{\mathrm{f}}(\tau_{\min})\le 0.5$, and $\tau_{\min}$ is just (34.g). As shown in fig. 7, the intersection of the two tangent lines refer to $\mathcal{B}_0(\gamma)$ of (33.a), and the solid, dash and dash-dot curves refer to the $B(\tau,\gamma)$ of (25), the $\tilde{B}(\tau,\gamma)$ of (26) and the $\hat{B}(\tau,\gamma)$ of (27) respectively. Consequently, the height of the intersection of the two tangent lines that contact the solid curve at τ_1 and τ_2 respectively is surely greater than the peak of this curve. Thus, $\mathcal{B}_0(\gamma)$ of (33.a) is justified to be an upper bound of $B_0(\gamma)$ of (30). Thus, the projection of the maximum of $\hat{B}(\tau,\gamma)$ on $\tilde{B}(\tau,\gamma)$ just represents the $\tilde{B}_0(\gamma)$ of (31). Consequently, we have that $B'_\tau\left(\acute{\tau}^{(i-1)},\gamma\right)\le B'_\tau\left(\dot{\tau}^{(i)},\gamma\right)\le B'_\tau\left(\grave{\tau}^{(i-1)},\gamma\right)$ and $B'_\tau\left(\acute{\tau}^{(i)},\gamma\right)\to 0_-$, $B'_\tau\left(\grave{\tau}^{(i)},\gamma\right)\to 0_+$ if $\mathrm{i}\to\infty$ is identical to $B'_\tau\left(\dot{\tau}^{(i)},\gamma\right)\to 0$ or $\mathcal{B}_0(\gamma)=B\left(\dot{\tau}^{(i)},\gamma\right)\to B_0(\gamma)$ if $i\to\infty$. Therefore, it is concluded.

APPENDIX C
THE PROOF OF PROPOSITION 3

Proof: According to the CLT, $\left(t(\mathbf{Y}|\mathcal{H}_1)-\mu_{\mathcal{H}_1}\right)/\sigma_{\mathcal{H}_1}$ will arbitrarily approach the distribution of $\mathcal{N}(0,1)$ provided that the cardinality of $\mathbf{Y}$ is sufficiently large. In other words,

$$y_{\mathcal{H}_1}=\left(t(\mathbf{Y}|\mathcal{H}_1)-\mu_{\mathcal{H}_1}\right)/\sigma_{\mathcal{H}_1}\vec{\sim}\mathcal{N}(0,1)\quad\text{if } K\to\infty\qquad\text{(C.1)}$$

where $\mu_{\mathcal{H}_1}$ and $\sigma_{\mathcal{H}_1}$ are given by (A.2) and (A.6), respectively, while the sign '$\vec{\sim}$' denotes 'approaches the distribution of'. The '$\vec{\sim}$' still holds if integral operations are applied to the PDFs of both sides of (C.1), and it also holds if applied to the $t(\mathbf{Y}|\mathcal{H}_1)$ provided so that the integral variant takes a proper transformation. Therefore, we conduct these operations to the PDF of $t(\mathbf{Y}|\mathcal{H}_1)$ just as (13) does and to that of $\mathcal{N}(0,1)$. This results in

$$\Gamma_0(\kappa,\varepsilon_0/\theta)\to\mathrm{Q}\left(\left(\hat{\varepsilon}_0-\mu_{\mathcal{H}_1}\right)/\sigma_{\mathcal{H}_1}\right)\quad\text{if } K\to\infty\qquad\text{(C.2)}$$

where $\hat{\varepsilon}_0$ and $\varepsilon_0$have been explained for (20) and (14), respectively, and $\mathrm{Q}(\cdot)$ denotes the Q function.

Since both $\mathrm{Q}(\cdot)$ and $\Gamma_0(\cdot,\cdot)$ are monotonic and continuous functions [13], [23], the '$\to$' still holds if the inverse operations are applied to both sides of (C.2). This means that for a specified $p_{\mathrm{d}0}$, we have

$$[Q^{-1}(p_{\mathrm{d}0})\,\sigma_{\mathcal{H}_1}+\mu_{\mathcal{H}_1}]=\hat{\varepsilon}_0\to\varepsilon_0=\theta\Gamma_0^{-1}(\kappa,p_{\mathrm{d}0})\quad\text{if } K\to\infty\qquad\text{(C.3)}$$

Based on (C.3), (24) and (17), we have

$$\tilde{p}_{\mathrm{f}}\to p_{\mathrm{f}},\quad\text{if } K\to\infty\qquad\text{(C.4)}$$

Similarly, under $\mathcal{H}_0$, still based on the CLT, we have

$$y_{\mathcal{H}_0}=\left(t(\mathbf{Y}|\mathcal{H}_0)-\mu_{\mathcal{H}_0}\right)/\sigma_{\mathcal{H}_0}\vec{\sim}\mathcal{N}(0,1)\qquad\text{(C.5)}$$

where $\mu_{\mathcal{H}_0}$ and $\sigma^2_{\mathcal{H}_0}$ can employ the related formulae of the Gamma distribution [13], [23] to be derived, given by $\mu_{\mathcal{H}_0}=\sigma_z^2$, $\sigma^2_{\mathcal{H}_0}=\sigma_z^4/K$.

Along the same way in which (C.2) is derived, conditioned on (C.3), we have

$$\mathrm{Q}\left(\left(\hat{\varepsilon}_0-\mu_{\mathcal{H}_0}\right)/\sigma_{\mathcal{H}_0}\right)\to\Gamma_0\left(K,K\varepsilon_0/\sigma_z^2\right)\quad\text{if } K\to\infty\qquad\text{(C.6)}$$

Based on (C.6), (21) and (17), we have

$$\hat{p}_{\mathrm{f}} \to p_{\mathrm{f}} \quad \text{if } K \to \infty \tag{C.7}$$

Consequently, based on (C.4), (C.7), (30) and (31), this proposition holds.

APPENDIX D
THE PROOF OF PROPOSITION 4

Proof: Let the condition applicable to [1] labelled A describing that the received signal of the complex PSK experiences a path of line of sight (LOS) and is contaminated by CSCG distributed noise. Under condition A, [1, Formula (13)] defines its false alarm probability to be $p_{\mathrm{f}} = \mathrm{Q}\left(\alpha + \gamma\sqrt{f_s\tau}\right)$ where $\alpha = \mathrm{Q}^{-1}\left(p_{\mathrm{d0}}\right)\sqrt{2\gamma+1}$ as defined for (23). Let the condition of proposition 4 of this paper be labelled B. The change from condition A to B is equivalent to the replacement of p_{f} of [1, eq. (13)] by (22), (17) or (24) of this paper, which have distinct connotations as previously explained.

For (22), its proof is evident. Let us rewrite $\alpha = Q^{-1}\left(p_{d0}\right)\sqrt{\gamma^2/m + 2\gamma + 1}$ and substitute it into [1, eq. (13)]. All procedures of the relevant proofs will still go along in the same way as [1] does. For (17) or (24), it is not so obvious as (22)'s proof. However, the essences remain the same. Their main distinctions from (13) of [1] lie merely on the outermost operator of $\Gamma_0(\cdot)$ instead of $\mathrm{Q}(\cdot)$, and the internal parameter α being $\theta\Gamma_0^{-1}\left(\kappa, p_{d0}\right)\sqrt{\gamma^2/m + 2\gamma + 1}$ other than $Q^{-1}\left(p_{d0}\right)\sqrt{2\gamma+1}$. Despite these two differences, all corresponding proofs can still be conducted through the same approaches as [1] does.

APPENDIX E
APPROACH OF ACQUIRING THE PARAMETERS OF (36)

First, the value of formula (36) should equal to that of (28) at the starting end of the ith piece. Thus, this equation should be met. It is given by

$$\tilde{\tau}_0^i\left(r_i\right) = \tau_0\left(r_i\right). \tag{E.1}$$

Second, to ensure the continuity of the PDF at the boundaries of adjacent pieces, the 1st derivatives w. r. t. γ should be equal. The set of equations that should be satisfied are

$$\frac{\mathrm{d}\tilde{\tau}_0^i(\gamma)}{d\gamma}\Big|_{\gamma=r_i} = \frac{\mathrm{d}\tau_0(\gamma)}{d\gamma}\Big|_{\gamma=r_i}; \tag{E.2}$$

$$\frac{\mathrm{d}\tilde{\tau}_0^i(\gamma)}{\mathrm{d}\gamma}\Big|_{\gamma=r_{i+1}} = \frac{\mathrm{d}\tau_0(\gamma)}{\mathrm{d}\gamma}\Big|_{\gamma=r_{i+1}}. \tag{E.3}$$

An explicit form expression of $\mathrm{d}\tau_0(\gamma)/\mathrm{d}\gamma$ is unachievable based on (28), but it can be approximated by $\left(\tau_0(r_i+\Delta\gamma) - \tau_0(r_i)\right)/\Delta\gamma$ provided that $\Delta\gamma$ is set to be sufficiently small.

Consequently, solving such a set of equations yields the values of parameters of (36) that are given by

$$\beta_i = r_i; \tag{E.4}$$

$$\varepsilon_i = \log\frac{\frac{d\tau_0(\gamma)}{d\gamma}|_{\gamma=r_{i+1}}}{\frac{d\tau_0(\gamma)}{d\gamma}|_{\gamma=r_i}}/(r_{i+1}-r_i); \tag{E.5}$$

$$\alpha_i = \frac{(r_{i+1}-r_i)\frac{d\tau_0(\gamma)}{d\gamma}|_{\gamma=r_{i+1}}}{\varepsilon_i e^{\varepsilon_i}}; \tag{E.6}$$

$$\mu_i = -\alpha_i + \tau_0\left(r_i\right). \tag{E.7}$$

REFERENCES

[1] Y.-C. Liang, Y. Zeng, E. C. Y. Peh, and A. T. Hoang, "Sensing-throughput tradeoff for cognitive radio networks," *IEEE Trans. Wireless Commun.*, vol. 7, no. 4, pp. 1326–1337, Apr. 2008.

[2] E. C. Y. Peh, Y.-C. Liang, Y. L. Guan, and Y. Zeng, "Optimization of cooperative sensing in cognitive radio networks: A sensing-throughput tradeoff view," *IEEE Trans. Veh. Technol.*, vol. 58, no. 9, pp. 5294–5299, Nov. 2009.

[3] M. Cardenas-Juarez and M. Ghogho, "Spectrum sensing and throughput trade-off in cognitive radio under outage constraints over Nakagami fading," *IEEE Commun. Lett.*, vol. 15, no. 10, pp. 1110–1113, Oct. 2011.

[4] L. Luo and S. Roy, "Efficient spectrum sensing for cognitive radio networks via joint optimization of sensing threshold and duration," *IEEE Trans. Commun.*, vol. 60, no. 10, pp. 2851–2860, Oct. 2013.

[5] S. Zhang, H. Zhao, S. Wang, and J. Wei, "A cross-layer rethink on the sensing-throughput tradeoff for cognitive radio networks," *IEEE Commun. Lett.*, vol. 18, no. 7, pp. 1226–1229, Jul. 2014.

[6] X. Hong, J. Wang, C.-X. Wang, and J. Shi, "Cognitive radio in 5G: A perspective on energy-spectral efficiency trade-off," *IEEE Commun. Mag.*, vol. 52, no. 7, pp. 46–53, Jul. 2014.

[7] M. Simsek, A. Aijaz, M. Dohler, J. Sachs, and G. Fettweis, "5G-enabled tactile Internet," *IEEE J. Sel. Areas Commun.*, vol. 34, no. 3, pp. 460–473, Mar. 2016.

[8] H. Song, X. Fang, and L. Yan, "Handover scheme for 5G C/U plane split heterogeneous network in high-speed railway," *IEEE Trans. Veh. Technol.*, vol. 63, no. 9, pp. 4633–4646, Nov. 2014.

[9] G. Mastroianni and G. V. Milovanović, *Interpolation Processes-Basic Theory and Applications* (Springer Monographs in Mathematics). Berlin, Germany: Springer-Verlag, 2008, p. 145.

[10] M. Gasca and J. J. Maeztu, "On Lagrange and Hermite interpolation in R^k," *Numer. Math.*, vol. 39, no. 1, pp. 1–14, Feb. 1982.

[11] S. Khemiri, G. Pujolle, K. Boussetta, and N. Achir, "A cross-layer radio resource management in WiMAX systems," in *Quality of Service and Resource Allocation in WiMAX*. Rijeka, Croatia: InTech, 2012, pp. 147–174.

[12] L. Ding, T. Melodia, S. N. Batalama, J. D. Matyjas, and M. J. Medley, "Cross-layer routing and dynamic spectrum allocation in cognitive radio ad hoc networks," *IEEE Trans. Veh. Technol.*, vol. 59, no. 4, pp. 1969–1979, May 2010.

[13] D. Stirzaker, *Elementary Probability*. New York, NY, USA: Cambridge Univ. Press, 2003, pp. 114–137.

[14] J. D. Parsons, *The Mobile Radio Propagation Channel*. New York, NY, USA: Wiley, 1992, pp. 114–189.

[15] F. F. Digham, M.-S. Alouini, and M. K. Simon, "On the energy detection of unknown signals over fading channels," *IEEE Trans. Commun.*, vol. 55, no. 1, pp. 21–24, Jan. 2007.

[16] N. Bouhlel and A. Dziri, "Maximum likelihood parameter estimation of Nakagami-gamma shadowed fading channels," *IEEE Commun. Lett.*, vol. 19, no. 4, pp. 685–688, Apr. 2014.

[17] S. Krantz and H. Parks, *The Implicit Function Theorem*. New York, NY, USA: Springer-Verlag, 2002, pp. 93–115.

[18] E. Artin, *Galois Theory*. Moneola, NY, USA: Dover, 1998, pp. 21–67.

[19] *IEEE Standard for Local and Metropolitan Area Networks—Part 16: Air Interface for Fixed Broadband Wireless Access Systems—Amendment for Physical and Medium Access Control Layers for Combined Fixed and Mobile Operation in Licensed Bands*, IEEE Standard 802.16e, IEEE Standard 802.16 Working Group,Dec. 2005.

[20] E. K. P. Chong and S. H. Zak, *An Introduction to Optimization*, 3rd ed. Hoboken, NJ, USA: Wiley, 2008, pp. 101–104.

[21] H. Michiel, *Encyclopedia of Mathematics*. Dordrecht, The Netherlands: Kluwer, 1995, pp. 507–508.

[22] S. Al-Ahmadi and H. Yanikomeroglu, "On the approximation of the generalized-K distribution by a gamma distribution for modeling composite fading channels," *IEEE Trans. Wireless Commun.*, vol. 9, no. 2, pp. 706–713, Feb. 2010.
[23] Wolfram Research Inc., Champaign, IL, USA. (1998). *The Wolfram Functions Site*. [Online]. Available: http://functions.wolfram.com
[24] A. M. Mathai and H. J. Haubold, *Special Functions for Applied Scientists*. Berlin, Germany: Springer, 2008, pp. 67–69.
[25] G. Pocovi, K. I. Pedersen, B. Soret, M. Lauridsen, and P. Mogensen, "On the impact of multi-user traffic dynamics on low latency communications," in *Proc. Int. Symp. Wireless Commun. Syst. (ISWCS)*, Poznań, Poland, Sep. 2016, pp. 204–208.
[26] S. Ahmadi, *LTE-Advanced: A Practical Systems Approach to Understanding 3GPP LTE Releases 10 and 11 Radio Access Technologies*, 1st ed. Oxford, U.K.: Academic, 2014, p. 344.

BIN GU (M'18) received the B.Eng. degree in electromagnetic field and microwave technology from Xidian University, Xi'an, China, in 1989, and the M.Eng. degree in electronic and communication engineering from Southeast University, China, in 2007, where he is currently pursuing the Ph.D. degree in communications and information system with the National Mobile Communications Research Laboratory. He is also with the School of Electronic and Information Engineering, Nanjing College of Information Technologies, Nanjing, China, as a professor majoring in wireless communications. He is a main inventor of four wireless communication-related patents in China. His research interests include wireless networks resource allocation, cognitive radio, optimization, and so on.

TIECHENG SONG (M'12) received the B.S. degree in radio technology, and the M.S. and Ph.D. degrees in communication and information system from Southeast University, China, in 1989, 1992, and 2006, respectively. He became an Associate Professor and a Professor with the National Mobile Communications Research Laboratory, Southeast University, in 2000 and 2005 respectively. He has published five books and over 100 papers. He is a main inventor of over 20 patents in China. His research interests include cognitive radio, wireless sensor networks, and vehicle networks. He received four times of the Science and Technology Award from Jiangsu Province, China.

JING HU (M'07) was born in 1975. She received the Ph.D. degree in electronics engineering from Southeast University, China, in 2011. She is currently an Associated Professor with the National Mobile Communications Research Laboratory, Southeast University. Her research interests include cognitive radio, wireless sensor networks, and vehicle networks.

ZHENGQUAN LI received the B.S. degree from the Jilin University of Technology in 1998, the M.S. degree from the University of Shanghai for Science and Technology in 2000, and the Ph.D. degree in circuit and system from Shanghai Jiao Tong University in 2003. He is currently a Professor with Jiangnan University, China. He is also a Post-Doctoral Researcher with the National Mobile Communications Research Laboratory, Southeast University. His current research interests include operative communications and massive MIMO.

DAFEI SUN was born in Henan, China, in 1976. He received the B.S and M.S degrees from the Department of Mathematics, Henan University, China. He is currently pursuing the Ph.D. degree in information and communication engineering with the National Mobile Communications Research Laboratory, Southeast University, China. His research interest includes statistical signal processing and spectrum sensing.